# EVALUATION OF ACOUSTIC SHIELDING EFFECTS FROM A GENERIC GARTEUR HELICOPTER CONFIGURATION

Jianping Yin, Jianping.Yin@dlr.de, DLR (Germany)
Karl-Stephane Rossignol, Karl-Stephane.Rossignol@dlr.de, DLR (Germany)
Gabriel Reboul, gabriel.reboul@onera.fr, ONERA (France)
Frederic Mortain, Frederic.Mortain@onera.fr, ONERA (France)
Luigi Vigevano, Luigi.Vigevano@polimi.it, Politecnico di Milano (Italy)
Alex Zanotti, Alex.Zanotti@polimi.it, Politecnico di Milano (Italy)
Giuseppe Gibertini, Giuseppe.Gibertini@polimi.it , Politecnico di Milano (Italy)
Mattia Barbarino, M.Barbarino@cira.it, CIRA (Italy)
Claudio Testa, Claudio.Testa@cnr.it, CNR-INSEAN (Italy)
Giovanni Bernardini, G.Bernardini@uniroma3.it, Roma tre University (Italy)
Harry Brouwer, Harry.Brouwer@nlr.nl, NLR (Netherlands)

**Abstract**
This paper presents the activities in the GARTEUR Action Group HC/AG-24 to study the noise scattering of helicopter rotors in the presence of the fuselage. The focus of the Action Group is on the development and the validation of numerical prediction methods and on establishing an experimental data base for numerical validations. This paper will focus on the results from the wind tunnel and the numerical activities achieved in the last stage of the project. Shielding experiments were conducted in DLR's Acoustic Wind tunnel in Braunschweig (AWB) using point and rotor noise sources. The numerical methods used in the group include Boundary Element Method (BEM) for solving the Helmholtz equation and Computational AeroAcoustic method (CAA) for solving the linearized Euler equations. The acoustic scattering predictions are compared to test data.

## 1. INTRODUCTION

Helicopter noise reduction is a long-term objective of research by academia and helicopter industry in view of reducing the environmental impact of helicopters and extending the market to new civil applications. Both the main and the tail rotors (including Fenestron) of a helicopter are major sources of noise and contribute significantly to its ground noise footprint. Past research efforts were mainly concentrated on the helicopter rotor noise generation and reduction. Even though the scattering of noise generated by helicopter rotors has been recognized and may have a significant influence on the noise spectra and directivity, it has not been an extensive research effort towards the comprehension of the phenomenon. To further understand the helicopter noise propagation under the influence of the helicopter fuselage (acoustic installation effects), the GARTEUR Action Group HC/AG-24[1][2][3][4] was established. The objectives of this AG are (1) to develop and validate numerical prediction methods and (2) to generate a unique noise scattering database through wind tunnel tests using generic configurations. Partners of the AG are CIRA, CNR-INSEAN, DLR, NLR, ONERA, Politecnico di Milano (Polimi), and Roma TRE respectively. The activities are coordinated by DLR. In order to achieve the objectives of the proposed AG, the project is structured in two work packages. The partners are involved in (1) experimental activities, during which suitable databases are produced for the phenomenological understanding and code validations, (2) numerical activities aiming at both providing baseline indications for the set-up of the experiments, and enhancing and validating the employed commercial or in-house computational tools.

The GARTEUR AG24 shielding experiments were conducted in DLR's small-scale low-speed Acoustic Wind tunnel in Braunschweig (AWB)[9]. Acoustic wave scattering for generic configurations (various spheres and a generical helicopter model) were studied using two point-sources and one rotor source. The results from the first two campaigns and the related numerical simulations by the partners to validate their simulation tools are already reported in [2][3].

This paper will focus on the results from the third wind tunnel test and the numerical activities achieved in the last stage of the project. The experimental approach used in the acoustic scattering test, including the noise sources, the wind tunnel models, the acoustic instrumentation and the data reduction will be first presented. The methodologies applied in the numerical simulations by the partners will then be described and analyzed to point out their strength and weaknesses. The acoustic scattering predictions will be analyzed and compared either code to code or with available test results for different source positions, frequencies and geometries.

## 2. DESCRIPTION ON THE SCATTERING TEST SETUP

There were three test campaigns carried out during the project. The first two involved scattering tests for spheres with different diameters and materials using two different noise point-sources from DLR and

Presented at 47th European Rotorcraft Forum, United Kingdom, 7-9th September, 2021

ONERA[7][8]. The experiment of the third campaign involves acoustic wave scattering for a generical helicopter model using the same point-noise sources from DLR and ONERA and one rotor source from Polimi[5][6]. Figure 1 shows the test set up for the scattering test with 3 different sources, top: DLR laser, middle: ONERA SPARC and bottom: Polimi tail rotor. The helicopter model consists of an assembly of generic forms such as an ellipsoid fuselage and cylindrical tail boom. The GARTEUR AG24 shielding experiments were performed in the DLR Acoustic Wind tunnel in Braunschweig (AWB)[9]. The AWB has a cross section of (1.2×0.8)$m^2$. The open jet test section is known for its excellent flow quality and anechoic properties as well as its low background noise. Acoustic measurements were conducted using an inflow microphone. The inflow acoustic measurement plane was set at 400 mm below the axis of the fuselage.

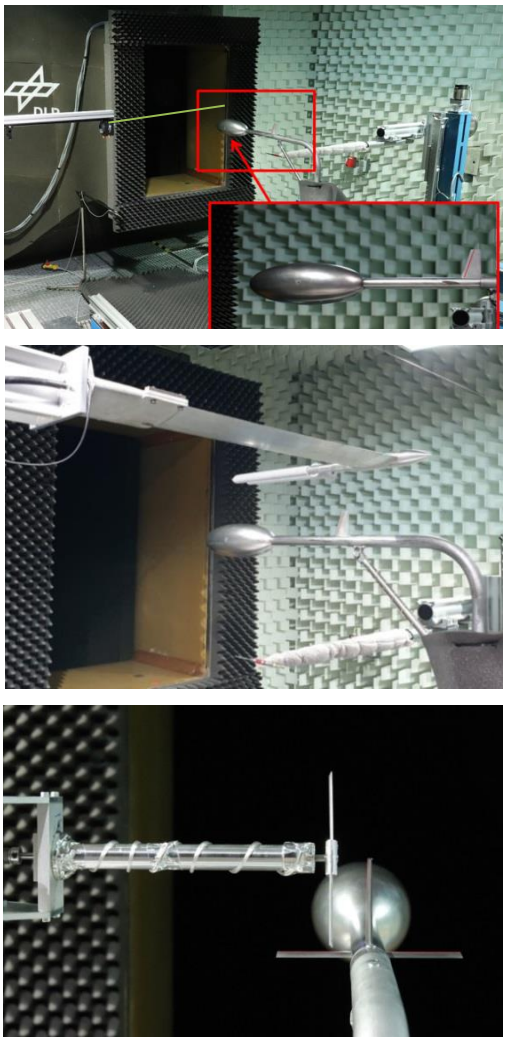

*Figure 1: Scattering experiments on a generic helicopter (Top: DLR laser point source; middle: ONERA SPARC source; Bottom: Polimi two blade tail rotor, looking upstream)*

The choice of the point noise sources is based on the criterion of non- or minimum-intrusiveness for both the mean flow and the scattered acoustic field. As shown in Figure 2, a detailed two point-source systems are used. The first one is an impulsive laser-based system from DLR and the other one is the SPARC system of ONERA. The optical setup for the DLR laser sound source is shown in Figure 2(a), where a combination of one concave lens and two convex lenses is applied to focus the laser beam onto a point inside the flow field about 500mm from the last convex lens. This initiates the impulsive formation of a small localized plasma and a pressure wave is formed which propagates through the surrounding medium. The SPARC system of ONERA, as shown in Figure 2 (b), consists of two sharp probes where the released energy of an abrupt current discharge is converted into heat in the small region between the probes and generates an acoustic pressure wave. Since the two noise sources have two different working frequency ranges, they complement each other to provide results in a wider frequency domain. The DLR laser sound source has the advantage of being non-intrusive for both mean flow and scattered acoustic field, while the ONERA SPARC source has a higher signal to noise ratio.

The third noise source used in the test is the rotor source from Polimi (Figure 1 bottom) consisting of a simplified double-blade tail rotor model. The rotor has a 0.075 m radius. The flat plate blades have 10 mm chord, 1.0 mm thickness and no twist. The blades are mounted to the hub with fixed pitch angles of 0° and 10°. Pitch setting can be reversed so that the rotor can operate either as a tractor or a pusher propeller. A Hall-effect sensor measures the number of revolutions per minute and is also the reference signal for the synchronization of the measurements. The tip Mach number (ISA) is about 0.54. The rotor is driven by a brush-less low-voltage electrical motor with an electronic controller. The main design criterion is that the generic rotor noise source should resemble the main characteristics of a tail rotor with the clear harmonic components of a rotor noise.

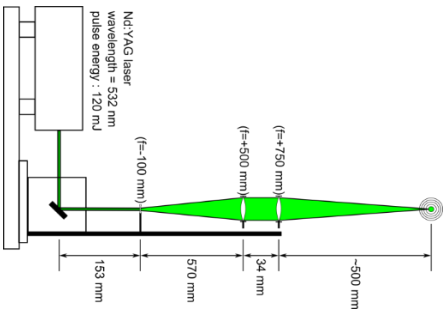


*(a) Optical setup for the laser sound source*

*(b) setup of the sharp probes from SPARC*

*Figure 2: A detailed two point-source systems*

For the data reduction of the measured acoustic signal of the point sources, the proper length of the temporal window is important to exclude the reflections from the wind tunnel, measurements mountings, microphone traverse and SPARC (arm). The analysis results indicate that the optimal length of the analysis window is about 3.4 ms for ONERA SPARC and about 0.8 ms for DLR laser sound source. In the acoustic signal processing of the rotor noise, averaging is required in order to increase the SN (Signal-to-Noise) ratio, and to reduce background noise as well as random noise. To derive the final spectrum for each microphone position, two averaging techniques were tested, time averaged and spectrum averaged. The difference of the spectrum- and time-averaged results can also be used to define the broadband noise in general. For the time averaging procedure, the 1/rev signal from the Hall-effect sensor is used, so that the time signal for a fixed number of revolutions is first overlapped and then averaged.

## 3. DESCRIPTION OF METHODOLOGIES APPLIED IN THE NUMERICAL SIMULATIONS BY THE PARTNERS

The numerical methods used in the action group include Boundary Element Methods (BEM) for solving the Helmholtz equation and Computational AeroAcoustic methods (CAA) for solving the linearized Euler equations. Table 1 summarizes the main characteristics of the codes used by the partners. Detailed descriptions of the methods can be found in[1][3][4]. For the BEM, both the Combined Helmholtz Integral Equation Formulation (CHIEF), Burton-Miller or Brakhage-Werner methods are used to treat the singularity and to remove the spurious frequencies. Based on the assumption of low Mach number potential flow, either a Taylor transformation of the convected wave equation method or applying convective green's function are used to consider the mean flow effect. In case of no mean flow, all BEM codes should provide the same level of the accuracy. However, the different treatment of mean flow effects may result in different predictions. All codes formulated within the context of BEM are suitable to propagate the acoustic waves to the far field. The Simulations provided in this paper involve only the results from BEM.

| | CIRA | DLR | NLR |
|---|---|---|---|
| Formulation | BEM | BEM | CAA |
| Treatment singularity | CHIEF | Burton-Miller | |
| Flow effect | Convective Green's function or nonlinear effect | Taylor transform | Included |
| Mesh | 2D unstructured | 2D unstructured | 3D structured |
| Acceleration | Fast multiple | Fast multiple | |
| Diffraction | yes | yes | yes |
| Domain | Frequency | Frequency | Time |

| | ONERA (1) | ONERA (2) | RomaTRE/CNR-INSEAN |
|---|---|---|---|
| Formulation | BEM | CAA | BEM |
| Treatment singularity | Brakhage-Werner | | CHIEF |
| Flow effect | Taylor transform | Included | Convective Green's function or nonlinear effect |
| Mesh | 2D unstructured | 3D structured | 2D structured |
| Acceleration | Adaptative Cross Approximation matrix | | No |
| Diffraction | yes | yes | yes |

*Table 1 Main Characteristics of the codes used by the partners*

## 4. RESULTS AND DISCUSSION

### 4.1. Fuselage scattering from noise source positions in the main rotor disc

In a first study noise source positions within the main rotor disc were tested. All tested main rotor point source positions (MPS, marked as solid circles) are shown in Figure 3 in both top and side view respectively. For validations of the numerical simulations, only two source positions, marked as 2 (MPS P2) and 3 (MPS P3) are chosen in this paper. The point source in MPS P3 position represents a possible main rotor BVI noise source position when operating in the descent flight. MPS P2 position is used to verify the measurement on the maximum possible scattering effect and the symmetry of the

scattering pattern. For the comparison of experimental and numerical results the shielding factor GT is evaluated. GT is defined as the ratio of total sound pressure and incident sound pressure. The advantage of using GT to evaluate the scattering effect is that no corrections on signal amplitude are required.

Measured contour plots of the shield factor in a receiving plan (microphones) at z=-0.4m using both DLR laser source (a) and ONERA SPARC (b) located at MPS P2, are shown in Figure 4 for two different frequencies. For a frequency near 2500 Hz the shielding factor is always less than one in the measurement area corresponding to an overall shadowing of the emitted noise. The strongest shadow regions are located on the port and starboard sides of the fuselage. The “silent zone” directly below the fuselage, where no incident wave can be propagated, is entirely determined by the diffracted waves, which have small peaks for this configuration, comparing to the other region. With increasing frequency, the shadow regions (blue area) become much stronger and shift slightly towards the fuselage. The diffracted waves cause a sound amplification (GT >1) on the edge of the measurement area for a frequency close to 5000Hz. For both measured frequency the experimental results obtained by the DLR laser source and ONERA SPARC are in good agreement.

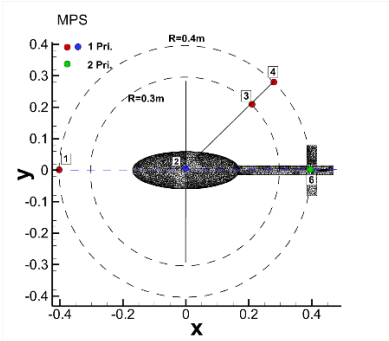


(a) Top view

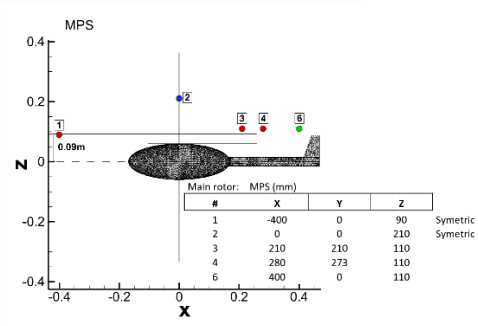


(b) Side view

*Figure 3: Positions of point source representing main rotor noise (MPS=Main rotor positions)*

Figure 5 shows simulated contour plots of shield factor from different partners for the same position as in Figure 4. As the size of the simulation area is slightly larger than in the tests, a rectangular dashed line in the numerical simulations was used to indicate the measurement area. There are very good correlations in terms of the general shielding characteristics and values with all numerical simulations. Since the carpet plot used in the numerical simulation is obtained with much more microphone positions than the experimental ones, the contour lines are smooth compared to the test. Slightly asymmetrical patterns were observed for all the frequencies in the test results, which may be caused by an influence of the asymmetry in the test setup, or the deviation of the source position from the symmetry plane.

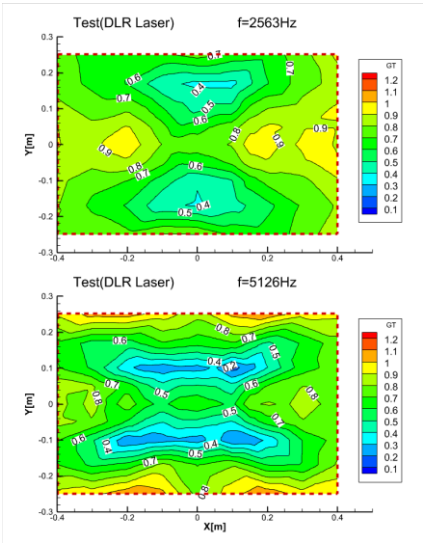


(a) Test results using DLR Laser

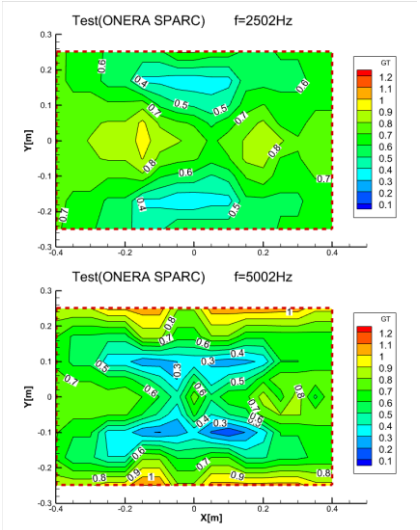


(a) Test results using ONERA SPARC

*Figure 4: Measured contour plot of shield factor for a point source at MPS P2 using DLR Laser and ONERA SPARC*

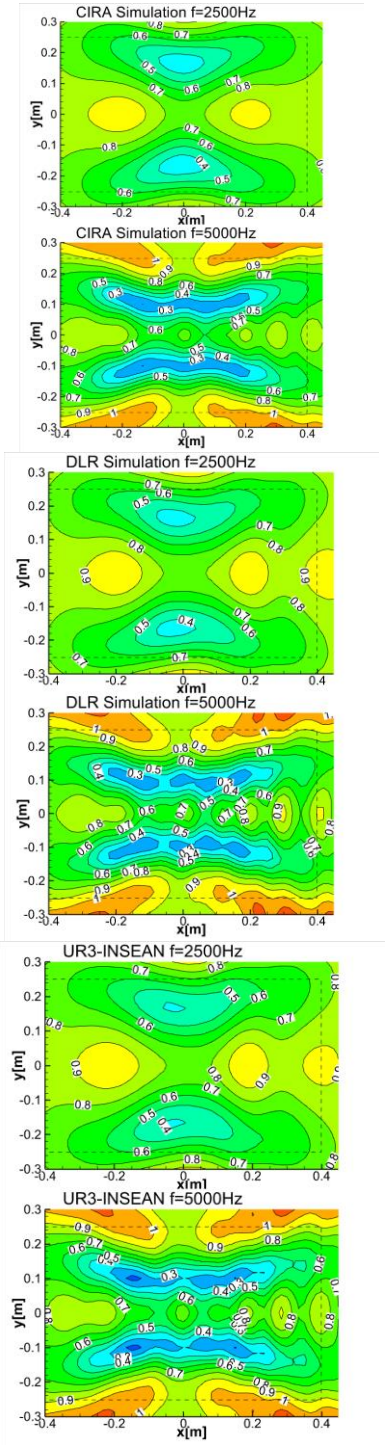


*Figure 5: Simulated contour plot of shield factor for a point source at MPS P2 by CIRA, DLR and UR3-INSEAN*

Measured contour plots of the shield factor GT using DLR laser source located at MPS P3 are given in Figure 6 for two different frequencies close to 2500 Hz and 5000 Hz respectively. In general, the complexity of the scattering pattern increases with increasing frequency. Test results also demonstrate an increased sound level in the area directly ahead of the fuselage, indicating the enhancement of the noise level instead of a cancelation for this source position. The numerical results for this source point are shown in Figure 7. There are again very good correlations in terms of the general shielding characteristics between experimental data and all the numerical predictions although there is a small underestimation in the values for f=2500Hz and a slight overestimation for f=5000Hz. In general, a cancelation of the sound waves (GT<1 area) below the fuselage is observed, but the shadowing is relatively weak compared with the source position MPS P2.

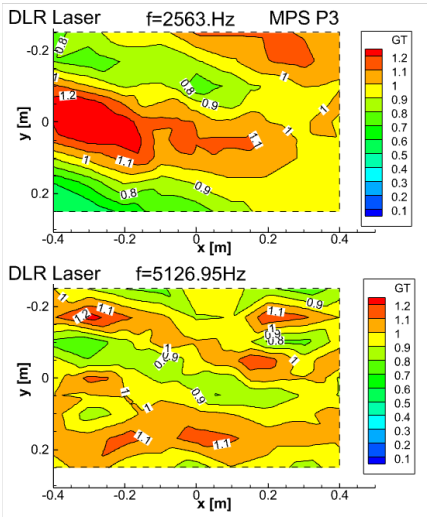


*Figure 6: Measured contour plot of shield factor for a point source at MPS P3 using DLR laser source*

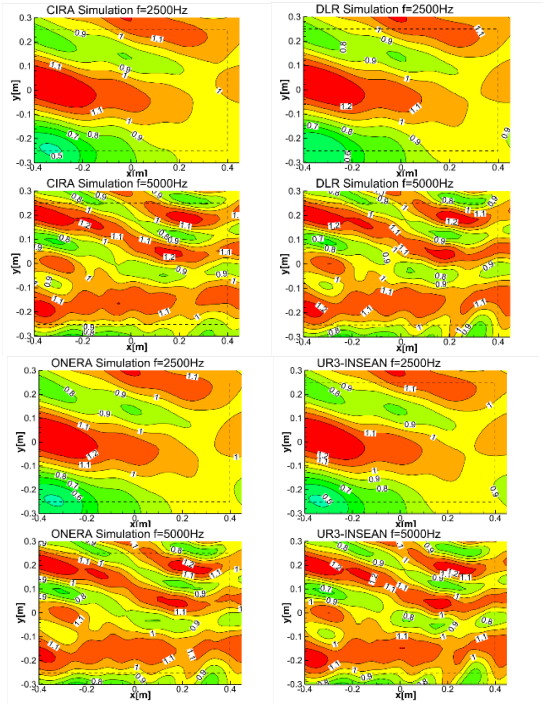


*Figure 7: Simulated contour plot of shield factor for a point source at MPS P3 by CIRA, DLR, ONERA and UR3-INSEAN*

### 4.2. Fuselage scattering from point source positions in the tail rotor disc

Point source positions representing tail rotor noise source position (TPS) were also tested. All tested TPS positions are shown in Figure 8 both top and side view respectively. For validations of the numerical simulations, only one source position, marked as 2 (TPS P2) is chosen.

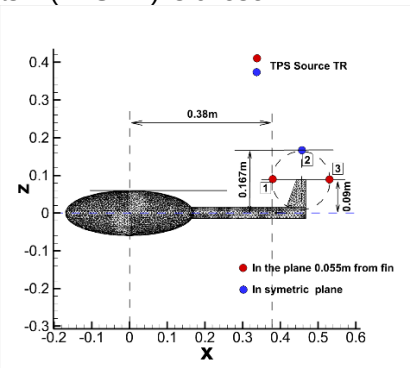


(a) Side view

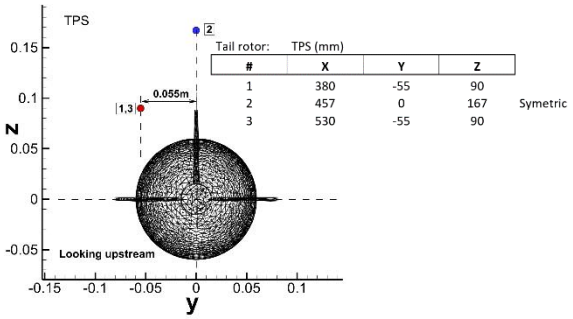


(a) Looking upstream

*Figure 8: Positions of point source representing tail rotor noise TPS*

Both the numerical simulations from CIRA&DLR&ONERA (Figure 10) and test results (Figure 9) show similar characteristics in the shielding patterns. The difference in the maximum and minimum values of GT is about ±0.05 within the measurement area marked by the rectangular dashed line in the numerical simulations. Very good correlations are achieved among the simulations.

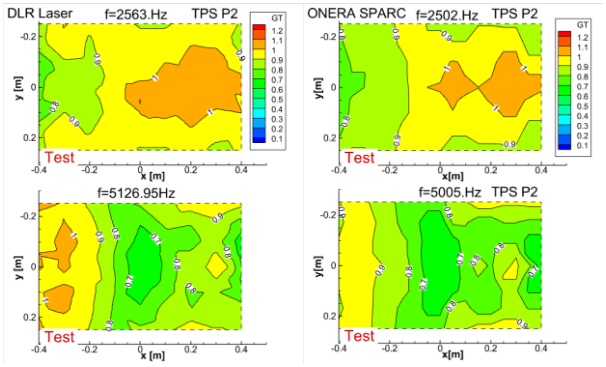


*Figure 9: Measured contour plot of shield factor for a point source at TPS P2 using DLR Laser and ONERA SPARC*

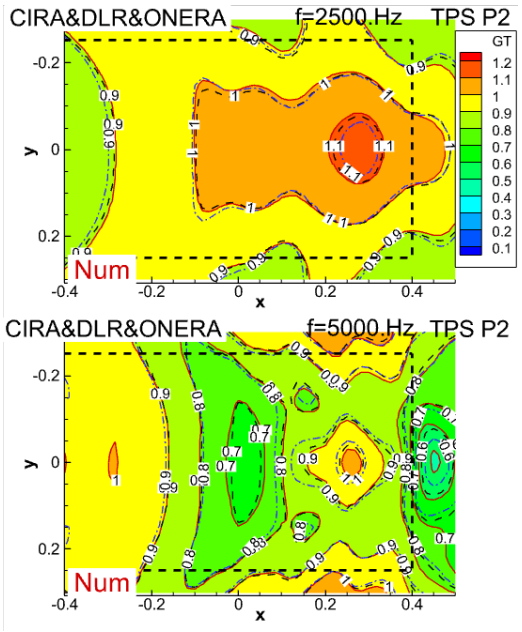


*Figure 10: Simulated contour plot of shield factor for a point source at TPS P2 (solid contour line DLR, dashed ONERA, dash-dot CIRA)*

### 4.3. Fuselage scattering of complete tail rotor noise

In previous sections the noise scattering for single source point positions within the main or tail rotor disc were analysed. In this section the noise scattering for the more realistic tail rotor model by Polimi will be studied. To predict the rotor noise scattering by the fuselage, the incident field of the rotor noise source is required. In the GARTEUR group, depending on the capability of each partner's code, two methodologies were used to derive the acoustic incident field, (1) the incident field was computed directly on the scattering body such as the fuselage by the Ffowcs Williams-Hawkings (FW-H) code using unsteady blade surface pressure provided by DLR; (2) the incident sound pressure field and its derivative is provided on a given Kirchhoff source surface around the tail rotor[10], as shown in Figure 11b. For

the first approach DLR computed the unsteady blade surface pressure using DLR's unsteady free wake 3-D panel code UPM (potential flow code). For the second approach the incident field on the Kirchhoff surface was computed with the DLR FW-H code APSIM using the unsteady blade pressure computed by UPM.

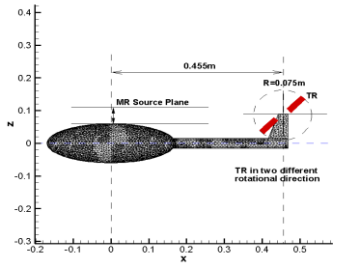


(a) Side view

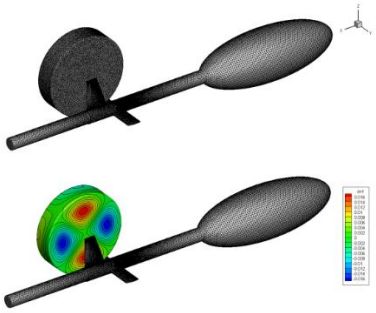

(b) Fuselage and source surface

*Figure 11: Top: geometric location of tail rotor source; Bottom: a Kirchhoff surface around the tail rotor for further simulation of the acoustic scattering*

The fuselage scattering of the rotor noise was tested for several rotor positions and two different rotor rotational directions[5][6]. Figure 12 and Figure 13 show the measured and the simulated contour plots of the shielding factor for the tail rotor noise scattering from the fuselage at three different tail rotor blade passing frequencies BPF1 (742 Hz), BPF2 (1484 Hz) and BPF3 (2225 Hz), respectively. For BPF1, the shadow region (marked by the arrow) on the starboard side of the fuselage is much larger in the test results compared to the numerical predictions. In addition, a hot spot appears in the test around x = -0.3 m for BPF3, which is not predicted in the simulations. A good agreement between the simulation and the test is found in terms of the position of both the shadow region pointed by the arrow and the enhancement region around the red dashed-dotted line in the plots. when compared with the point source cases, the agreement is not as satisfactory. There are several reasons which may be responsible for the discrepancy in the comparisons, such as the difference of real noise emission of the tail rotor in the test and the predicted noise emission based on numerical simulations of the tail rotor aerodynamics using a panel method. Finally, one can also pointed out once again the good agreement among the available numerical predictions.

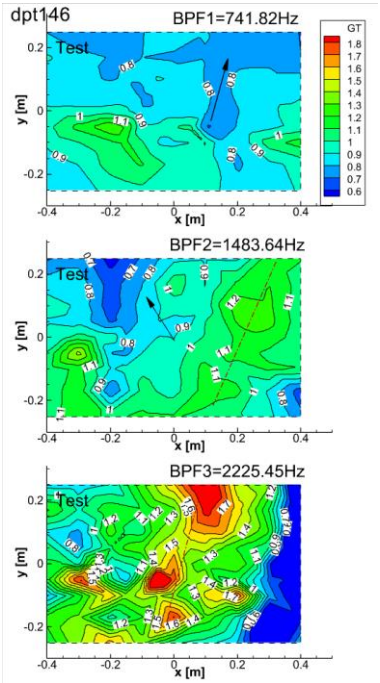


*Figure 12: : Measured contour plot of the shield factor for the fuselage-rotor noise scattering at blade passing frequencies BPF1, BPF2 and BPF3*

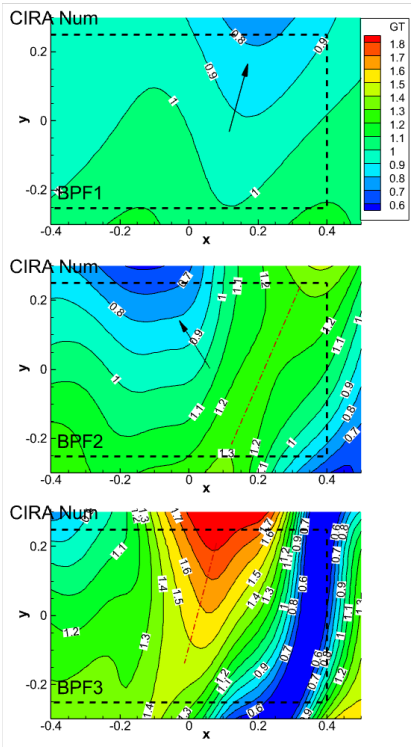


*(a) CIRA*

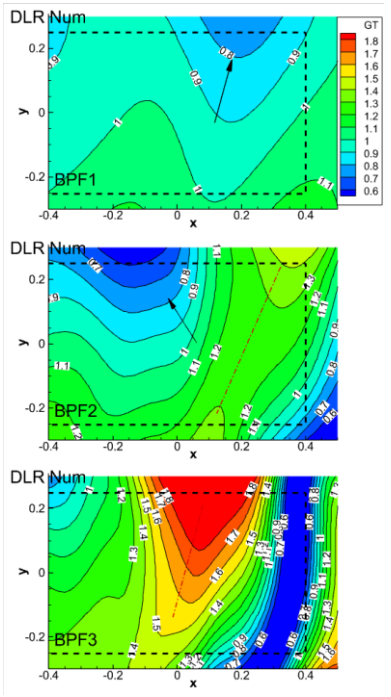


(b) DLR

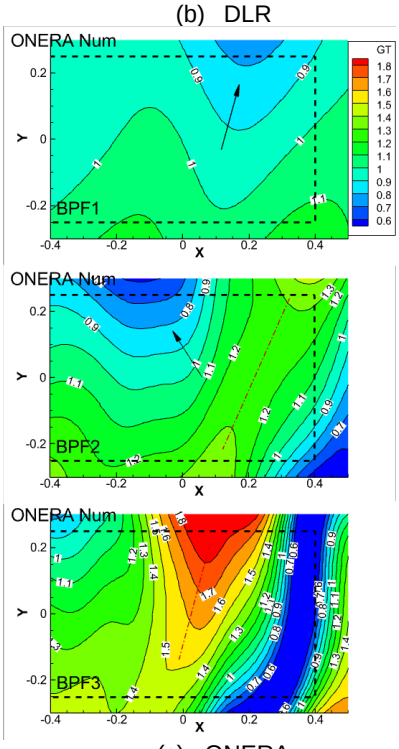


(c) ONERA

*Figure 13: Simulated contour plot of the shielding factor for the fuselage-rotor noise scattering using source surface incident field for the blade passing frequencies BPF1, BPF2 and BPF3. Computations by CIRA, DLR and ONERA.*

## 5. CONCLUSION REMARKS

In this paper, the wind tunnel test and the numerical activities achieved in the last stage of GARTEUR AG24 is introduced. The experimental and numerical investigations of the shielding characteristics of a generic helicopter fuselage are presented.

Comparisons of code-to-code and the code-to-test results were carried out. The test results are derived from the noise source generated from either a point or a rotor source. The numerical comparisons were conducted among different solvers available within GARTEUR Action Group AG24.

The following concluding remarks can be drawn:

i) Test results from both DLR laser-based and ONERA SPARC noise source capture the general characteristics of the noise shielding effect from a point monopole. For both measured frequency the experimental results obtained by the DLR laser source and ONERA SPARC are in good agreement.

ii) In case of the point source, very good correlations are achieved between experimental data and all the numerical predictions, both in terms of the general shielding characteristics and the scattering factors.

iii) The numerical simulation results for fuselage scattering using the point source indicate that the BEM method has a high level of accuracy. There are very good comparisons among all numerical simulations.

iv) A more realistic scattering situation was experimentally studied for a generic tail rotor. Numerical simulations showed an overall good correlation with experimental data, but the prediction accuracy was lower than for the point source.

## 6. ACKNOWLEDGMENTS

The research leading to the presented results has been addressed within the framework of the HC/AG-24 Helicopter Fuselage Scattering Effects for Exterior/Interior Noise Reduction, supported by GARTEUR.

## 7. REFERENCES

[1]. Barbarino, M. und Bianco, D. und Yin, J. und Lummer, M., Reboul, G., Gennaretti, M., Bernardini, G., Testa, C., “Acoustical methods towards accurate prediction of rotorcraft fuselage scattering”, 42nd European Rotorcraft Forum, September 5-8, Lille, France, Paper 62, 2016

[2]. Yin, J. und Rossignol, K-S. und Bulté, J., “Acoustic scattering experiments on spheres for studying helicopter noise scattering”, 42nd European Rotorcraft Forum, September 5-8, Lille, France, Paper 127, 2016

[3]. Yin, J., Rossignol, K-S., Barbarino, M., Bianco, D., Testa, C., Brouwer, H., Janssen, S-R., Reboul, G., Vigevano, L., Bernardini, G., Gennaretti, M., Serafini, J., Poggi, C., “Acoustical methods and experiments for studying rotorcraft fuselage scattering”, 43rd European Rotorcraft Forum, September 12-15, Milan, Italy, 2017
[4]. Yin, J., Rossignol, K-S., Barbarino, M., Bianco, D., Testa, C., Brouwer, H., Janssen, R., Reboul, G., Vigevano, L., Bernardini, G., Gennaretti, M., Serafini, J., Poggi, C., “GARTEUR activities on acoustical methods and experiments for studying on acoustic scattering”. CEAS Aeronautical Journal, Vol 10 (2), Page 531-551, 2019 (DOI: 10.1007/s13272-018-0333-0)
[5]. Gibertini, G. and Zanotti, A (POLIMI): “Calibration tests of the tail rotor model at Politecnico di Milano, AG24 Report 2017
[6]. Yin, J., Zanotti, A., Rossignol, K-S., Gibertini, G., Vigevano, L., “Design of a generic rotor noise source for helicopter fuselage scattering tests”, 44rd European Rotorcraft Forum, Delft, The Netherlands 18-21 September 2018.
[7]. Karl-Stéphane Rossignol, Jan Delfs, and Fritz Boden., "On the Relevance of Convection Effects for a Laser-Generated Sound Source", 21st AIAA/CEAS Aeroacoustics Conference, AIAA-Aviation,(AIAA2015-3146). http://dx.doi.org/10.2514/6.2015-3146.
[8]. P. Lebigot, J. Bulté, R. Davy, F. Desmerger, L. Coste, "SPARC: Source imPusionnelle AéRoACoustique", ONERA Technical Report (in French), N°4/22699, 2015.
[9]. M. Pott-Pollenske, J. W. Delfs, “Enhanced Capabilities of the Aeroacoustic Wind Tunnel Braunschweig”, 14th AIAA/CEAS Aeroacoustics Conference (29th AIAA Aeroacoustics Conference), 2008, AIAA-2008-2910
[10]. Yin, J., “Investigation of Rotor Noise Shielding Effects by the Helicopter Fuselage in Forward Flight”, Journal of Aircraft, 56 (4), page 1-12. American Institute of Aeronautics and Astronautics (AIAA). doi: 10.2514/1.C035009. ISSN 0021-8669, July 2019.